



Fine mapping and candidate gene analysis of $qSB12^{YSB}$, a gene conferring major quantitative resistance to rice sheath blight

Yu Wang¹ · Quanyi Sun¹ · Jianhua Zhao¹ · Taixuan Liu¹ · Haibo Du¹ · Wenfeng Shan¹ · Keting Wu¹ · Xiang Xue^{4,5} · Chao Yang⁶ · Jun Liu⁶ · Zongxiang Chen^{1,2} · Keming Hu^{1,2} · Zhiming Feng^{1,2} · Shimin Zuo^{1,2,3}

Received: 23 March 2023 / Accepted: 7 October 2023 / Published online: 16 November 2023
© The Author(s), under exclusive licence to Springer-Verlag GmbH Germany, part of Springer Nature 2023

Abstract

Key message $qSB12^{YSB}$, a major quantitative sheath blight resistance gene originated from rice variety YSBR1 with good breeding potential, was mapped to a 289-Kb region on chromosome 12.

Abstract Sheath blight (ShB), caused by *Rhizoctonia solani* Kühn, is one of the most serious global rice diseases. Rice resistance to ShB is a typical of quantitative trait controlled by multiple quantitative trait loci (QTLs). Many QTLs for ShB resistance have been reported while only few of them were fine-mapped. In this study, we identified a QTL on chromosome 12, in which the $qSB12^{YSB}$ resistant allele shows significant ShB resistance, by using 150 BC₄ backcross inbred lines employing the resistant rice variety YSBR1 as the donor and the susceptible variety Lemont (LE) as the recurrent parent. We further fine-mapped $qSB12^{YSB}$ to a 289-kb region by generating 34 chromosomal segment substitution lines and identified a total of 18 annotated genes as the most likely candidates for $qSB12^{YSB}$ after analyzing resequencing and transcriptomic data. KEGG analysis suggested that $qSB12^{YSB}$ might activate secondary metabolites biosynthesis and ROS scavenging system to improve ShB resistance. $qSB12^{YSB}$ conferred significantly stable resistance in three commercial rice cultivars (NJ9108, NJ5055 and NJ44) in field trials when introduced through marker assisted selection. Under severe ShB disease conditions, $qSB12^{YSB}$ significantly reduced yield losses by up to 13.5% in the LE background, indicating its great breeding potential. Our results will accelerate the isolation of $qSB12^{YSB}$ and its utilization in rice breeding programs against ShB.

Introduction

Rice sheath blight (ShB), caused by *Rhizoctonia solani* Kühn (*R.solani*), is one of the most devastating diseases in rice worldwide. Under intensive and high-input production system and favorable conditions, ShB can cause up to 50% of grain yield losses (Cu et al. 1996; Lee and Rush 1983). These intensified systems rely heavily on the use of high-yielding, semi-dwarf rice varieties, high crop densities, and high rate of nitrogen fertilizers. All these factors make ShB a major constraint for rice production in Asia, America, and other rice-growing areas (Gnanamanickam 2009; Savary et al. 1995). Spraying fungicides has been the major approach to control ShB because of very few rice varieties with complete or high resistance to ShB, which severely hinders the progress on developing ShB resistant varieties. A few germplasms, like Tetep, Jasmine 85,

Teqing and YSBR1, were reported to carry good resistance to ShB (Channamallikarjuna et al. 2010; Pan et al. 1999; Zuo et al. 2009). Among them, YSBR1, derived from an inter-subspecies rice hybrid, showed high-level, stably reliable ShB resistance at stages from seedling to adult plants and in different environments, including field, growth chamber and greenhouse (Zuo et al. 2009). Most recently, YSBR1 was found to significantly suppress *R. solani* hypha growth through the observation of *R. solani* hyphal behavior on the surface of leaf sheaths (Cao et al. 2022).

The current breeding practice has been using varieties with certain levels of resistance to ShB, namely quantitative resistance controlled by quantitative trait loci (QTLs) (Li et al. 1995a; Zou et al. 2000). To date, more than 50 ShB resistance, QTLs have been preliminarily mapped on all rice 12 chromosomes (Molla et al. 2020), and some of them, have been validated, such as $qSB-9^{TQ}$, $qSB-11^{LE}$, $qSB11-1$, $qSB-11^{HIX}$, $qSB9-2$, $qSB-7^{TQ}$ (Li et al. 1995a; Eizenga et al. 2015; Molla et al. 2020; Zhu et al. 2014). However, due to the fact that many factors, such as the micro-climates, canopy density, plant height and heading date, may disturb

Communicated by Joshua N. Cobb.

Extended author information available on the last page of the article

the phenotyping of ShB disease, only a very few ShB resistance QTLs have been fine mapped so far. To decrease these afflictions and enhance the accuracy of phenotypic evaluation, further improving the phenotypic evaluation method and developing specific mapping population have been recommended, which led to the successfully fine mapping of *qSB-9^{TQ}* and *qSB-11^{LE}*. The *qSB-9^{TQ}* was mapped into a 146-kb region, and 12 candidates were identified (Zuo et al. 2014). Eleven genes in a 78.87-kb region were identified as the most likely candidates for *qSB-11^{LE}* (Zuo et al. 2013). To date, no ShB QTLs were successfully characterized, which has, to a great extent, hindered the utilization of ShB QTLs in the breeding against the disease.

It is known that *R. solani* secretes host-specific toxins, cell wall degrading enzymes, and effectors as weapons to counter rice defense, while in turn rice uses diverse strategies to fight against it. Host defense strategies mainly include phytohormone signaling, pathogenesis-related proteins (PR), antimicrobial compounds and secondary metabolites (Li et al. 2021; Molla et al. 2020). Besides these universal defense-response genes/compounds in host–pathogen interactions, some specific components have been identified either. For example, Li et al. (2019b) recently identified a F-box protein ZmFBL41 conferring ShB resistance in maize, and its homologous gene *OsFBX61* in rice also negatively regulated ShB resistance by targeting and degrading ZmCAD, a lignin biosynthesis enzyme. Loose Plant Architecture 1 (LPA1) interacts with a kinesin-like protein (KLP) to promote rice resistance to ShB via activation of PIN-FORMED 1a (PIN1a)-dependent auxin redistribution and subsequent activation of auxin signaling (Chu et al. 2021). Tissue-specific activation of DOF11 promotes both rice ShB resistance and grain yield through the activation of SWEET14 (Kim et al. 2021). Reactive oxygen species (ROS) appears to have dual roles as it is benefit for *R. solani* infection but also involved in plant basal defense responses (Foley et al. 2016; Shetty et al. 2008). OsRSR1 and OsRLCK5 are involved in ShB resistance by regulating host ROS contents induced by *R. solani* through the glutathione (GSH)-ascorbic acid (AsA) antioxidant system (Wang et al. 2021). Overexpression of *OsNYC*, a chlorophyll degradation gene, significantly enhances ShB susceptibility by inhibiting ROS scavenging processes (Cao et al. 2022). The *qLN11* ShB resistance QTL was considered to involve in the activation of genes associated with the ROS-redox pathway and alleviates ROS accumulation in rice, thus delaying *R. solani* colonization (Oreiro et al. 2022). However, the molecular mechanisms underlying the rice–*R. solani* interaction remain unclear and the breeding potential of these genes remain inadequate.

In this study, we fine-mapped an ShB resistance QTL *qSB12^{YSB}*, which carries a good breeding potential, and preliminarily analyzed its possible resistance mechanism. We repeatedly evaluated the phenotypes of 34 chromosomal

segment substitution lines (CSSLs) derived from YSBR1 and Lemont (LE) cross using three inoculation methods in two years, and finally fine-mapped *qSB12^{YSB}* to a 289-kb region on chromosome 12. Through the integration analysis of transcriptomic and resequencing data, we identified 18 candidate genes for *qSB12^{YSB}* and found that *qSB12^{YSB}* may activate secondary metabolites biosynthesis and ROS scavenging system to enhance rice ShB resistance.

Materials and methods

Plant materials

Rice variety YSBR1, developed by pedigree breeding from the progeny of a Japonica/Indica hybrid, carries a reliable high resistance to rice ShB evaluated by several methods in different locations and years (Zuo et al. 2009). LE, a japonica rice cultivar from Louisiana, USA, demonstrates high susceptibility to ShB (Bollich et al. 1985; Li et al. 1995b). The CSSL P5585 line carrying increased ShB resistance was identified in a set of backcross lines between LE (the recipient parent) and YSBR1 (the donor parent). P5585 was backcrossed with LE (recurrent parent) to generate a segregating BC₄F₂ population for primary QTL mapping. One BC₄F₂ line sharing, the same genetic background with LE but contains a YSBR1 chromosomal segment over the region between markers RM28553 and RM28819 was selected to generate a set of BC₅F₃ lines for fine mapping of *qSB12^{YSB}*. Simultaneously, a near-isogenic line, NIL-*qSB12^{YSB}* (CSSL-25), which harbored only a short chromosomal segment containing *qSB12^{YSB}* from YSBR1, was selected for RNA-seq analysis. NJ9108, NJ5055, and NJ44, commercial rice cultivars widely planted in Jiangsu province for their premium eating quality, all are susceptible or highly susceptible to ShB (Li et al. 2019a; Wang et al. 2007, 2012, 2013). All plants were grown in the experimental fields of Yangzhou University in Yangzhou (Jiangsu, China) under normal cultivation conditions.

Fungal inoculation and phenotyping of rice ShB tolerance

YN-7, a *R. solani* AGI-1A isolate with strong pathogenicity, was used in inoculation assays. The YN-7 strain was inoculated on potato dextrose agar (PDA) medium and cultured at 28 °C for 3 days. Mycelial discs (ca. 0.7 cm in diameter) were transferred to potato dextrose broth (PDB) medium containing autoclaved veneers (1.0 cm long × 0.3 cm wide × 0.8 mm thick) and grown at 28 °C until mycelia twined around the veneers. The veneers with mycelia were used as the inoculum.

All plants were grown in the field in Yangzhou (Jiangsu, China) and evaluated for ShB resistance by three different methods, adult plant inoculation in the field, adult plant inoculation in greenhouse and detached tiller inoculation in growth chamber.

Adult plant inoculation in the field: Rice plants at late tillering stage were inoculated by inserting the wood inoculum colonized with *R. solani* into the inside of the third leaf sheath from the top. Each plant was inoculated on three largest tillers. Disease severity was rated at around 30 days after heading using a '0~9' ShB rating system (Zuo et al. 2013). The disease score of each rice line/variety was calculated by averaging the disease score of 24 plants from three replications.

Adult plant inoculation in greenhouse: Rice plants at late tillering stage were selected and transplanted to a long plastic basin in a greenhouse with controlled humidity (45%–60%) and temperature (30°C/13 h, 26°C/11 h). Each basin contains 5 rice plants as one replication. Five tillers in each plant were inoculated as described above. The lesion length of each plant was measured at 14 days after inoculation (DAI). The average lesion length of 15 plants from three replications was used to represent the lesion length of the corresponding line or variety.

Detached tiller inoculation in a growth chamber was done as described by He et al. (2020). A single tiller was detached from the plant and fixed on flower mud. Leaves of the tiller were trimmed. The wood inoculum colonized with *R. solani* was inserted into the inside of 2nd leaf sheath from the top. All inoculated sheathes were placed on an inoculation shelf with controlled temperature and humidity, then the lesion length was measured at 7 DAI. Each rice variety or line was inoculated at least 20 sheathes separated in two to three inoculation shelves. The experiment was repeated two times. Two-tailed student's *t*-tests were used for comparison between two groups. Data are presented as mean (average) \pm sd. $P < 0.05$ was considered to be statistically significant.

Primer design and QTL mapping

For fine-mapping of *qSB12^{YSB}*, we developed 142 polymorphic markers, including SSR (simple sequence repeat) markers and Indel (insertion and deletion) markers. SSR markers and Indel markers were designed based on the sequence differences obtained from resequencing results of YSBR1 and LE. Sequences of Indel primers are listed in Supplemental table 2.

The phenotypic values of ShB resistance of the 150 BC₄F₂ CSSLs from field test were used to detect QTLs by biparental populations module (BIP) packaged within Ici-Mapping 4.2.

DNA extraction and resequencing

Genomic DNA from rice plants was extracted using young leaves with the CTAB (hexadecyltrimethylammonium bromide) method described by Porebski et al. (1997). The extracted DNA yield and purity were measured using a Nanodrop (Thermo Fisher Scientific) and visualized in a 1.2% agarose gel after electrophoresis. After the quality of genomic DNA samples was confirmed, DNA resequencing was conducted by Huazhi Biotech Co. Ltd. Raw reads were filtered to obtain clean reads to ensure the quality of subsequent information analyses. The sequencing reads were compared with the reference genome and relocated to the reference genome for subsequent analysis.

RT-qPCR and RNA-seq assays

Sheathes were collected at indicated time points in 1.5 ml RNase free centrifuge tubes and frozen in liquid nitrogen. Total RNA was extracted by the Trizol method (Invitrogen) and genomic DNA digested by DNase I (TaKaRa). Then, RT-qPCR assays were performed with SYBR Green reagent (Takara) on the CFX96™ Real-Time PCR Detection System (Bio-Rad, Hercules, CA) to detect specific genes. The level of actin mRNA was used as a standard control to normalize relative transcript levels. Primers used for RT-qPCR are listed in Supplemental Table 1. For candidate genes analysis, the relative expression levels of each gene in LE and NIL-*qSB12^{YSB}* in 0 and 20 HAI were analyzed.

For RNA-seq analysis, sheathes of 8-week-old rice plants 0 and 20 HAI were collected. RNA integrity was evaluated using the Agilent 2100 Bioanalyzer (Agilent Technologies). Samples with an RNA integrity number of ≥ 7 were processed for the subsequent analysis. RNA sequencing was conducted by OE Biotech. Transcriptomic profiling was performed according to the standard protocol of the Affymetrix Rice Genome Array (CapitalBio). Differentially expressed genes were selected using $|\text{Log}_2 \text{Fold change}| \geq 1$ and $q\text{-value} < 0.05$ as the cutoffs. Hierarchical cluster analysis of differential expression genes was performed to examine transcript expression patterns. Heat map and KEGG pathway enrichment analysis of differential expression genes were performed using the R package.

Enzymatic activity assay

In order to determine the activity of superoxide dismutase (SOD), glutathione S-transferase (GST), ascorbate peroxidase (APX), catalase (CAT), the infected and un-infected plant sheathes were sampled and measured using SOD, GST, APX and CAT Activity Assay Kit (Beijing Solarbio Science & Technology Co.,Ltd).

Table 1 The candidate genes in *qSB12^{YSB}* region

Gene	Expression type		Expression level after inoculation				Have dif- ferences in promoter or 3' UTR	Have non- synonymous mutation in CDS	Annotation
	RNA-seq	RT-qPCR	LE		NIL- <i>qSB12^{YSB}</i>				
			Expression level	Fold change	Expression level	Fold change			
Os12g0612500	DEG	DEG	–	–0.30	Down	–0.94*	Yes	No	Methyltrans- ferase small domain containing protein
Os12g0612700	IG	IG	Down	–3.17*	Down	–3.90*	Yes	Yes	Class III Homeodo- main Leucine Zipper Gene
Os12g0613200	EG	DEG	–	0.38	Down	–1.76*	Yes	Yes	SET domain group protein
Os12g0613700	EG	DEG	–	–0.11	Up	0.80*	Yes	No	Auxin response factor ARF25
Os12g0614000	EG	EG	–	–0.67	Down	–1.54*	Yes	Yes	Mediator com- plex protein OsMED19a
Os12g0614050	EG	EG	–	–0.34	–	–0.12	Yes	Yes	Hypothetical protein
Os12g0614900	EG	DEG	–	–0.03	Down	–1.03*	Yes	No	OsWAK127b— OsWAK short gene, expressed
Os12g0615200	DEG	DEG	Up	1.08*	Down	–1.98*	Yes	No	OsWAK129c— OsWAK receptor-like protein kinase
Os12g0615300	DEG	DEG	Up	1.59*	–	–0.01	Yes	No	OsWAK129b— OsWAK receptor-like protein kinase
Os12g0615400	DEG	DEG	–	–0.40	Down	–3.77*	Yes	Yes	Methyltrans- ferase domain containing protein
Os12g0615600	DEG	DEG	Up	1.25*	–	–0.13	Yes	No	PPR repeat- containing protein
Os12g0615800	EG	EG	–	–0.03	–	–0.08	Yes	Yes	G-patch domain- containing protein
Os12g0616000	DEG	DEG	–	–0.10	Down	–1.05*	Yes	Yes	Kinesin motor domain- containing protein
Os12g0616200	EG	DEG	–	–0.40	Down	–1.43*	Yes	No	Ribosomal protein
Os12g0616500	EG	DEG	Up	1.26*	–	0.48	Yes	No	Similar to cation proton exchanger
Os12g0616600	DEG	DEG	–	–0.19	Down	–0.94*	Yes	No	Putative Deg protease homologue

Table 1 (continued)

Gene	Expression type		Expression level after inoculation				Have differences in promoter or 3' UTR	Have non-synonymous mutation in CDS	Annotation
	RNA-seq	RT-qPCR	LE		NIL- <i>qSB12</i> ^{YSB}				
			Expression level	Fold change	Expression level	Fold change			
Os12g0616800	EG	EG	–	–0.51	–	–0.56	No	Yes	Protein of unknown function DUF761
Os12g0616900	DEG	DEG	Down	0.79*	Up	1.04*	Yes	Yes	Transketolase

* $P < 0.05$ using Student's *t*-tests

Evaluation of agronomic traits in the field

Rice lines were planted in 3 rows per line in the field with three replications. Each row contained 12 plants. Under slight-disease conditions, the rice lines were sprayed chemical fungicides thifluzamide during the tillering, jointing, booting and full heading stage. Under severe-disease conditions, 5 tillers per plant were inoculated with *R. solani* and didn't spray any fungicides.

The middle 10 plants in the central row were selected for measuring agronomic traits at the maturing stage. Various agronomic traits such as plant height, tiller number, tiller angle, heading date, panicle length, flag leaf length, flag leaf width, 1000 grain weight, grain length and width, panicle number per plant, grain number per main panicle, number of filled grains were measured as described (Chen et al. 2014). Seed-setting rate was calculated as: (Total number of filled grains per main panicle/total number of grains per main panicle) × 100%. The average value of the 10 plants represents the value of this rice line.

To measure grain yields of LE and NIL-*qSB12*^{YSB} in slight-disease and severe-disease conditions, each line was planted with three replications in the field; each replication contains 10 rows. Grain yields were determined when the seeds were harvested and normalized to yield per 10 000 m² (hm²).

Results

Preliminary mapping of *qSB12*^{YSB}

We previously generated several advanced backcrossing (BC₄) lines using YSBR1 as the donor and LE as the recipient parent. In a ShB nursery field, we found that line P5585 showed the highest resistance to ShB. To further confirm its resistance, we then artificially inoculated this line with *R. solani* in the field and found that its average disease scores were 5.08, significantly lower than that of LE (score = 6.81)

(Fig. 1a). Heading date and morphological traits, including plant height and tiller angle, have been found to be tightly associated with ShB resistance (Srinivasachary and Savary 2011). Therefore, we measured these traits plus tiller number, flag leaf length and width for both LE and line P5585. The results showed that P5585 and LE significantly differed only in plant height, and P5585 (105 cm) was significantly higher than LE of 96 cm (Fig. 1b). To eliminate the interference of plant height on the resistant phenotype of P5585, we further evaluated its ShB resistance by detached tiller inoculation assay, in which the sheath on detached tiller was inoculated in a growth chamber, and adult plant inoculation method in green house under controlled temperature and humidity. We found that P5585 showed an average lesion length of 9.13 cm, significantly shorter than LE of 13.75 cm, in the detached tiller inoculation assay (Fig. 1c). Because this assay excludes the effect from plant height, it indicates that the taller plant height of P5585 is not responsible for its stronger ShB resistance. Inoculation of the adult plants displayed a similar trend as the detached tiller results (Fig. 1d). Taken together, we conclude that the ShB resistance of P5585 is reliable and mainly not from the indirect effect of plant height.

We subsequently analyzed the genetic background of P5585 using 142 polymorphic molecular markers that differentiate between YSBR1 and LE (Supplemental Fig. 1). The results showed that P5585 and LE differed on 15 SSR loci and 7 of them concentrated on the end part of chromosome 12. The remaining 8 SSR markers located on 5 chromosomes, with 2 on each of chromosome 1, 3 and 6, and 1 on each of chromosome 2 and 10. To preliminarily determine the location of the resistance gene and simultaneously eliminate background affection, we backcrossed P5585 with LE to construct a BC₅F₂ population consisting of 150 plants. We firstly inoculated these plants artificially in the green house and then conducted a QTL linkage analysis using the phenotype data and genotype data on 142 polymorphic markers of each plant. A significant logarithm of odds (LOD) peak than the threshold value of 2.5 was detected

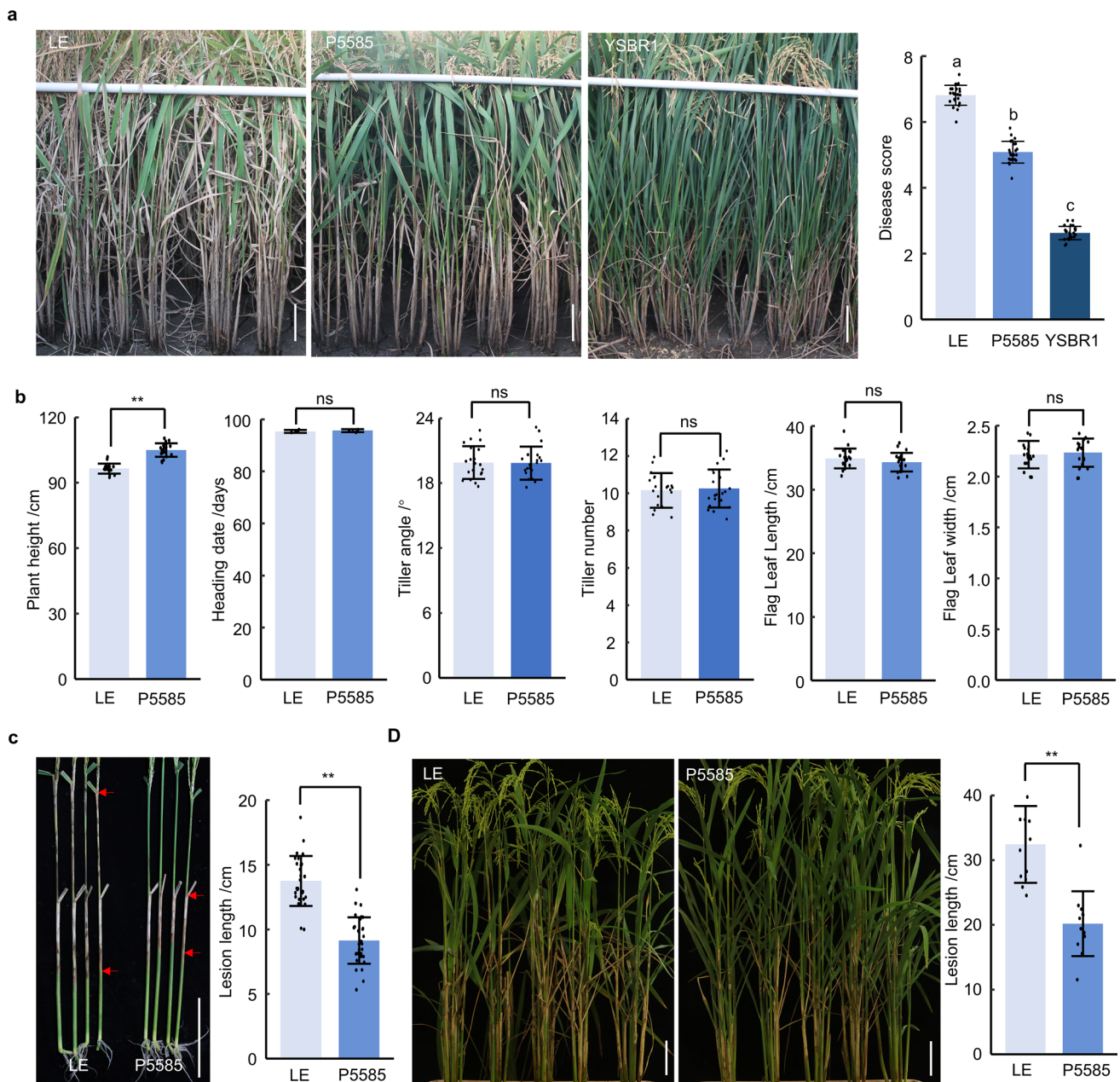


Fig. 1 Sheath blight resistance and agronomic traits of P5585. **a** Disease phenotype of LE, P5585 and YSBR1 after ShB inoculation under field conditions. Disease score was determined at 40 days after inoculation (DAI). Values are means \pm SD ($n=24$ plants). Different letters represent significant differences, $P<0.05$, one-way ANOVA. Scale bar, 10 cm. **b** Agronomic traits of LE and P5585 under field conditions. Plant height, heading date, tiller angle, tiller number, flag leaf length and flag leaf width were measured at maturing stage. Values are means \pm SD ($n=20$ plants). Heading date were scored in three replications. Values are means \pm SD ($n=3$). **, $P<0.01$; ns, not sig-

nificant using Student's t -tests. **c** Disease phenotype of LE and P5585 after ShB inoculation on sheath in a detached tiller. Single tillers from 8-week-old plants were detached, leaves trimmed and sheaths inoculated with *R. solani*. Lesion lengths were measured at 7 DAI. Values are means \pm SD ($n=30$). **, $P<0.01$ using Student's t -tests. Scale bar, 10 cm. **d** Disease phenotype of LE and P5585 inoculated in green house. Lesion length was measured at 14 DAI. Values are means \pm SD ($n=12$ plants). **, $P<0.01$ using Student's t -tests. Scale bar, 5 cm

on the end of chromosome 12 (Fig. 2a), indicating an ShB resistance QTL located in this region. No QTL was inferred on other polymorphic markers or regions. Based on the linkage map, we named this ShB resistance QTL as $qSB12^{YSB}$

hereafter and found it most likely located in the interval of markers RM28553 and RM28819 covering 3.35 Mb on the rice physical map.

Fine mapping of *qSB12^{YSB}*

In order to further narrow down the region of *qSB12^{YSB}*, we selected one BC₅F₂ plant, which shares the same genetic background to LE but carries an YSBR1 chromosomal segment over the *qSB12^{YSB}* region, to self-pollenate to develop lines carrying contiguous substitution segments in this region. Seven new polymorphic markers in the *qSB12^{YSB}* region were developed and used to determine the recombinants by marker-assisted selection (MAS). In the BC₅F₃ generation, we obtained 34 chromosomal segment substitutional lines (CSSLs), in which the contiguous and overlapping YSBR1 segments completely cover the *qSB12^{YSB}* region between markers RM28553 and RM28819 (Fig. 2b). At least one cross-over point was found between adjacent markers in these 34 CSSLs, except between markers RM6306 and RM28819. The average marker intervals of 10 markers were 372 kb, which led to a relatively high resolution for further mapping of *qSB12^{YSB}*.

We repeatedly evaluated the ShB resistance of the 34 CSSLs using three different methods in 2021 and 2022. We found that most lines showed consistent phenotypes with different methods in different years. A few lines showed ambiguous phenotypes in one method, which did not significantly affect the determination of their phenotypes because their phenotypes were consistent in two other methods. We then determined the phenotype of each of the 34 CSSLs and classified them into two clusters according to their disease scores or ratings (Supplemental Fig. 2). We also evaluated the plant height of these CSSLs and found no association between plant height and ShB resistance (Fig. 2b), which further confirmed that *qSB12^{YSB}* against ShB resistance was not caused by the indirect effect of plant height.

We found that all CSSLs containing the YSBR1 segment over the region between Ind25.916 and Ind26.205 showed significantly higher resistance than LE, indicating that this region co-segregated with *qSB12^{YSB}*. Eight CSSLs had crossovers in the Ind25.916~Ind26.205 region, and all these CSSLs contained an YSBR1 segment covering Ind26.205 but not Ind25.916. Moreover, while CSSLs-23 and 24 were susceptible, the other CSSLs displayed a relatively resistant phenotype. This indicates that Ind25.916 is the left border and Ind26.205 is the right border of *qSB12^{YSB}* (Fig. 2b). Finally, we fine mapped the *qSB12^{YSB}* to the region between Ind25.916 and Ind26.205 covering 289 kb in length on the rice physical map.

Determination of the candidate genes for *qSB12^{YSB}*

In the rice genome annotation database, 43 putative genes were annotated in the *qSB12^{YSB}* region. We compared the

sequences of the 43 genes between YSBR1 and LE after whole genome resequencing and found 423 SNPs/Indels between YSBR1 and LE in 39 genes. Among them, 287 SNPs/Indels exist in the upstream untranslated regions (UTRs) or promoters and 34 SNPs in coding sequences (CDSs) with 22 of them causing amino acid changes. These SNPs/Indels potentially contribute to the *qSB12^{YSB}* phenotype.

We also performed RNA-seq analysis on LE and CSSL-25 (hereafter namely NIL-*qSB12^{YSB}*) with or without *R. solani* infection and analyzed the expression patterns of these 43 genes in LE and NIL-*qSB12^{YSB}* after inoculation. We compared the RNA-seq and RT-qPCR data for the candidate genes and a few randomly selected genes and found a consistent trend between the two data, indicating the reliability of RNA-seq data (Supplemental Fig. 3).

We corrected the expression patterns of 5 candidate genes according to their RT-qPCR results (Table 1). Finally, the transcriptomic and resequencing data were combined and visualized in Fig. 3. Among the 43 genes, 16 genes did not express in either inoculated or not (No expression genes, n) and were therefore ruled out. Total of 14 genes were induced by *R. solani* differentially between LE and NIL-*qSB12^{YSB}* (Differential expression genes, DEGs), and 13 of them harbor SNPs/Indels in UTRs or promoters. Twelve genes expressed in the corresponding region of *qSB-12^{YSB}* (Expression genes, EGs), which were not induced by *R. solani* infection, and 4 of them harbor a nonsynonymous mutation in CDS. One gene harbors a nonsynonymous mutation in CDS and was induced by *R. solani* but no differential expression between LE and NIL-*qSB12^{YSB}* (Induced expression gene, IEG). Therefore, these 18 genes, 1 IEG, 13 DEGs and 4 EGs, were candidate genes for *qSB12^{YSB}*.

The expression levels of these 18 candidate genes in LE and NIL-*qSB12^{YSB}* at 0 and 20 h after inoculation are shown in Fig. 3. Most of these genes encode proteins with a known domain or predicted function as described below (Table 1): methyltransferase small domain containing protein (Os12g0612500), class III homeodomain leucine zipper gene (Os12g0612700), SET domain group protein (Os12g0613200), auxin response factor (Os12g0613700), nucleolar protein NOP5 (Os12g0614000), Hypothetical protein (Os12g0614050), OsWAK127b (Os12g0614900), OsWAK129c (Os12g0615200), OsWAK129b (Os12g0615300), methyltransferase domain-containing protein (Os12g0615400), PPR repeat-containing protein (Os12g0615600), G-patch domain-containing protein (Os12g0615800), kinesin motor domain-containing protein (Os12g0616000), ribosomal protein (Os12g0616200), similar to cation-proton exchanger (Os12g0616500), putative Deg protease homologue (Os12g0616600), protein of

Fig. 2 Fine mapping of *qSB12^{YSB}*. **a** LOD graph for the detection of sheath blight resistance QTLs on chromosome 12 by inclusive composite interval mapping in BC₃F₂ (P5585 × LE). **b** A diagram for the genotypes and resistance phenotypes of CSSLs and controls. Dark blue and light blue bars represent YSBR1 and LE chromosomal segments, respectively. Horizontal red line represents the fine mapping region of *qSB12^{YSB}*. Vertical lines represent the marker positions. 2021 and 2022 represent inoculations done in years 2021 and 2022. Field, GH, and DT represent whole plants inoculated in the field, whole plants inoculated in a greenhouse, and single tillers inoculated in a growth chamber, respectively. Pink and green blocks represent highly susceptible and partially resistant phenotypes, respectively. Yellow blocks represent taller plant heights than LE and light blue blocks indicate LE height

unknown function DUF761 (Os12g0616800), transketolase (Os12g0616900).

Resistant line NIL-*qSB12^{YSB}* shows stronger ability on scavenging ROS than susceptible Lemont after the infection of *R. solani*

Based on our RNA-seq data, we found 2594 and 5384 *R. solani*-induced/suppressed genes in LE and NIL-*qSB12^{YSB}*, respectively (Supplement Fig. 4a). Cluster analysis grouped these genes into 11 significantly enriched gene clusters (Fig. 4a). KEGG enrichment analysis was performed for each cluster. Clusters 2 and 6 were either upregulated or downregulated in LE and NIL-*qSB12^{YSB}*; the upregulated genes were enriched in the biosynthesis of secondary metabolites, metabolic pathways, MAPK signaling pathway, alpha-linolenic acid metabolism or plant hormones signal transduction whereas the downregulated genes were enriched in photosynthesis. The specifically upregulated genes in NIL-*qSB12^{YSB}* (cluster 7) were enriched in the biosynthesis of secondary metabolites, the biosynthesis of amino acids, glutathione metabolism and phenylpropanoid biosynthesis. In addition, the activation of glycolysis pathway has been reported accompanied with the activation of phenylpropanoid pathway to produce resistance-related secondary metabolites (Mutuku and Nose 2012). We found that compared with susceptible lines, infected resistant line NIL-*qSB12^{YSB}* has higher expression levels of genes in these pathways, suggesting that NIL-*qSB12^{YSB}* may produce more resistance-related antioxidants to defend *R. solani* (Supplemental Fig. 4c).

According to previous reports showing that *R. solani* induces plant cell death rapidly (Anderson et al. 2016). Enhancing the ability of plant cells to maintain redox homeostasis may significantly suppress *R. solani* growth (Oreiro et al. 2022). We therefore analyzed the genes in cell redox homeostasis pathways in LE and NIL-*qSB12^{YSB}*

after inoculation and identified 38 ROS scavenging-related proteins (Fig. 4b), including peroxiredoxins, glutathione reductase (GSR), glutathione peroxidase (GRX), ascorbate peroxidase (APX), glutaredoxin, disulfide isomerase (PDI), catalase (CAT), superoxide dismutase (SOD), glutathione S-transferase (GST). Most of them were upregulated in NIL-*qSB12^{YSB}* upon *R. solani* infection but only few were upregulated in LE (Fig. 4b). Furthermore, we measured the activities of these enzymes, SOD, GST, APX and CAT, and as expected, we observed that three enzymes of them (SOD, GST, APX) showed apparently higher levels in NIL-*qSB12^{YSB}* than those in LE after inoculation of *R. solani* (Supplemental Fig. 4b). We also observed that the downregulated genes in NIL-*qSB12^{YSB}* were enriched in carbon fixation (Cluster 4). The deceleration of carbon fixation will free reducing power (in the form of NADPH) to cope with *R. solani*-induced oxidants, thereby favoring ROS scavenging (Michelet et al. 2005, 2006, 2013; Schürmann and Buchanan 2008). Ribulose-1,5 biphosphate carboxylase/oxygenase (Rubsico), phosphoglycerate kinase (PGK), glyceraldehyde-3-phosphate dehydrogenase (GAPDH) are main genes involved in carbon fixation. Most of these genes were downregulated in NIL-*qSB12^{YSB}* but not in LE, suggesting the downregulation of the Calvin Benson cycle in NIL-*qSB12^{YSB}* (Fig. 4c). In higher plants, the oxidative pentose phosphate pathway (OPPP) is also a major source of reducing power (Scharte et al. 2009). We did observed that upregulation of the pentose phosphate pathway was more specifically in NIL-*qSB12^{YSB}* (Fig. 4d). The DAB (3,3-Diaminobenzidine) staining result verified that NIL-*qSB12^{YSB}* accumulated apparently less ROS than LE (Fig. 4e). Taken together, these data suggest that resistant NIL-*qSB12^{YSB}* has stronger ability to counter ROS bursts induced by *R. solani* than susceptible LE.

qSB12^{YSB} displays stably resistant effects in different rice varieties

To determine the resistant effects of *qSB12^{YSB}* in different rice varieties, we further introduced *qSB12^{YSB}* by MAS into three commercial rice varieties, NJ9108, NJ5055 and NJ44. These three varieties have been widely planted in Jiangsu province, China, with over 306 million hectares in total. In the BC₂F₃ generation, we obtained at least two lines in each variety background. These lines were evaluated together with their corresponding controls for ShB resistance in both field and green house conditions. The results (Fig. 5a–c) showed that the *qSB12^{YSB}*-containing lines in all three genetic backgrounds showed significantly lower disease scores than their corresponding controls in the field. In

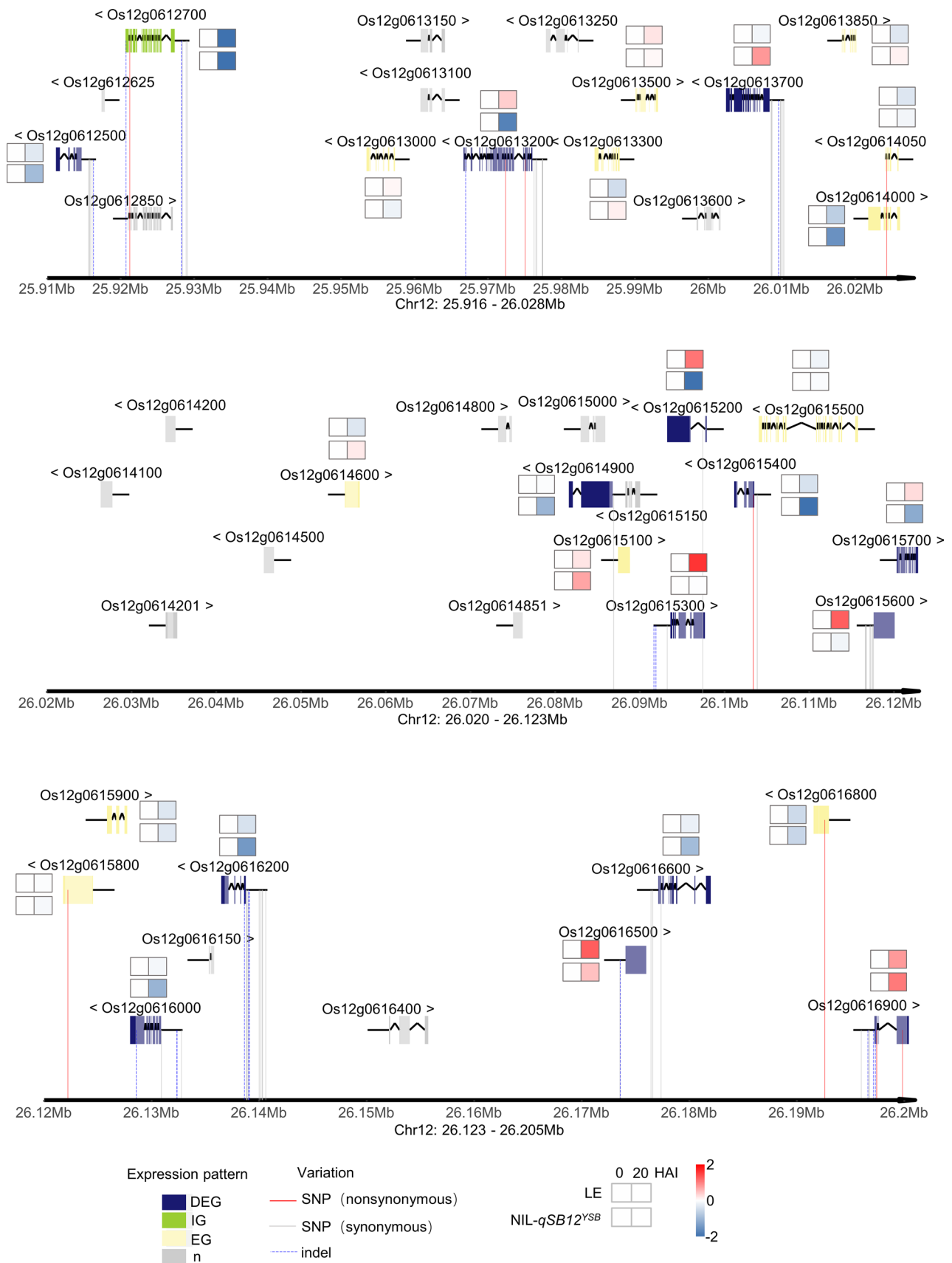


Fig. 3 Putative genes in the $qSB12^{YSB}$ region. Dark blue, green, yellow and gray blocks represent the genes induced by *R. solani* differentially between LE and NIL- $qSB12^{YSB}$ (DEG), genes induced by *R. solani* but no differential expression between LE and NIL- $qSB12^{YSB}$ (IG), genes expressed but not induced by *R. solani* (EG), non-expression genes (*n*), respectively. Red line, light grey line, and blue dashes represent nonsynonymous SNPs, synonymous SNPs, and Indels, respectively. The heat maps besides a gene represent the expression levels of this gene in LE (upper) and NIL- $qSB12^{YSB}$ (lower) in 0 and 20 h after inoculation (HAI)

average, the $qSB12^{YSB}$ reduced disease scores by 1.17–2.02 in different genetic backgrounds. Similar results were found in green house inoculations. These data clearly demonstrate that $qSB12^{YSB}$ is able to improve ShB resistance in the three commercial rice varieties.

To further evaluate the breeding potential of $qSB12^{YSB}$, we measured the yields of LE and NIL- $qSB12^{YSB}$ under slight-disease and severe-disease conditions in field trials (Fig. 5d). The results showed that in slight-disease condition, LE and NIL- $qSB12^{YSB}$ had similar grain yields (Fig. 5e). However, NIL- $qSB12^{YSB}$ performed significantly better than LE in severe-disease condition: While LE suffered a 25.3% yield loss compared with slight-disease, NIL- $qSB12^{YSB}$ only sustained an 11.8% loss under severely diseased condition. Plant yield is comprised by tiller number (TN), grain number per panicle (GNP), ratio of filled grains (RFG) and 1000-grain weight (1000GW), we then further analyzed these traits in these trials. The results showed that no significant differences were found in these traits between LE and NIL- $qSB12^{YSB}$, except for the ratio of filled grains (RFG) (Fig. 5e). While LE sustained a 25.6% loss in RFG, NIL- $qSB12^{YSB}$ sustained only a 10.1% loss in RFG under severe-disease condition, representing a 60% improvement in preventing RFG loss by $qSB12^{YSB}$. Therefore, the rescued yield losses by $qSB12^{YSB}$ is mainly attributed to the reduction in RFG loss. Taken together, we conclude that $qSB12^{YSB}$ can retrieve about 13.5% (25.3%–11.8%) of the yield losses caused by *R. solani* by mainly reducing the loss in RFG.

Discussion

Comparison of the location of $qSB12^{YSB}$ with previous studies and its breeding potential

Here, we identified an ShB resistance QTL from the resistant YSBR1 variety and fine-mapped it to a 289-kb

region between 25.916 and 26.205 Mb on chromosome 12 in the physical map. To date, a total of 7 independent studies have identified the existence of ShB resistance QTLs on chromosome 12 (summarized in Supplemental Table 2 and Supplemental Fig. 5). However, among these ShB QTLs, almost no was repeatedly detected in different years or in different environments, except $qSBD-12-2(E1)$ and $qSBPL-12(E2)$. $qSB12^{YSB}$ is located on the end of the long arm of chromosome 12, in or around the two previously identified QTLs, $qSB-12$ and $qRTL12$ (Supplemental Fig. 5) (Pinson et al. 2005; Taguchi-Shiobara et al. 2013). So far, fine-mapping of $qSB12$ has not been reported, which hinders the utilization of this QTL in breeding practice.

Using a pair of NILs in the LE background, we found that compared with LE, the NIL- $qSB12^{YSB}$ decreased 13.5% yield losses in severe ShB disease condition, indicating a great potential of $qSB12^{YSB}$ in rice breeding against ShB. Furthermore, we introduced $qSB12^{YSB}$ into three commercial varieties (NJ9108, NJ5055 and NJ44) with different genetic backgrounds, and confirmed that $qSB12^{YSB}$ did significantly improve the ShB resistance of *Japonica* rice. Besides, we also found different degrees of increased plant height in these lines compared with their respective recurrent parents. However, we did not find an association between $qSB12^{YSB}$ -conferred ShB resistance and plant height. There are significant differences between YSBR1 and the three commercial varieties in plant height, which might be due to residual YSBR1 chromosomal segments in the background of these BC₂F₃ lines that lead to the increased plant height. We will continue to backcross the BC₂F₃ lines to their recurrent parents to exclude the interference of other chromosomal segments in the future.

Candidate genes and resistance mechanisms of $qSB12^{YSB}$

Based on the transcriptomic and resequencing data, we comprehensively compared the expression patterns and sequence variations of the genes in the $qSB12^{YSB}$ fine mapping region and ultimately inferred 18 most likely candidates for $qSB12^{YSB}$. To further determine the priority of these candidate genes for next step verification test, the functions of these genes were discussed, which allowed us to consider the following 10 genes that would be of higher priority for functional verification: *Os12g0613700*,

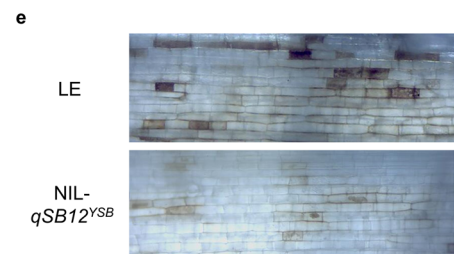
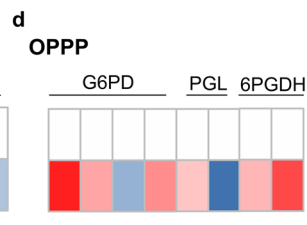
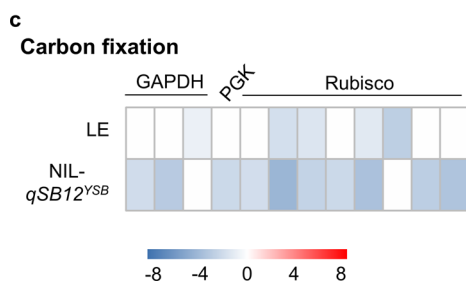
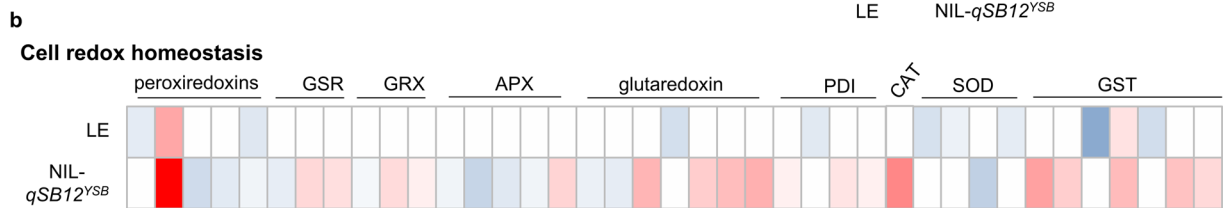
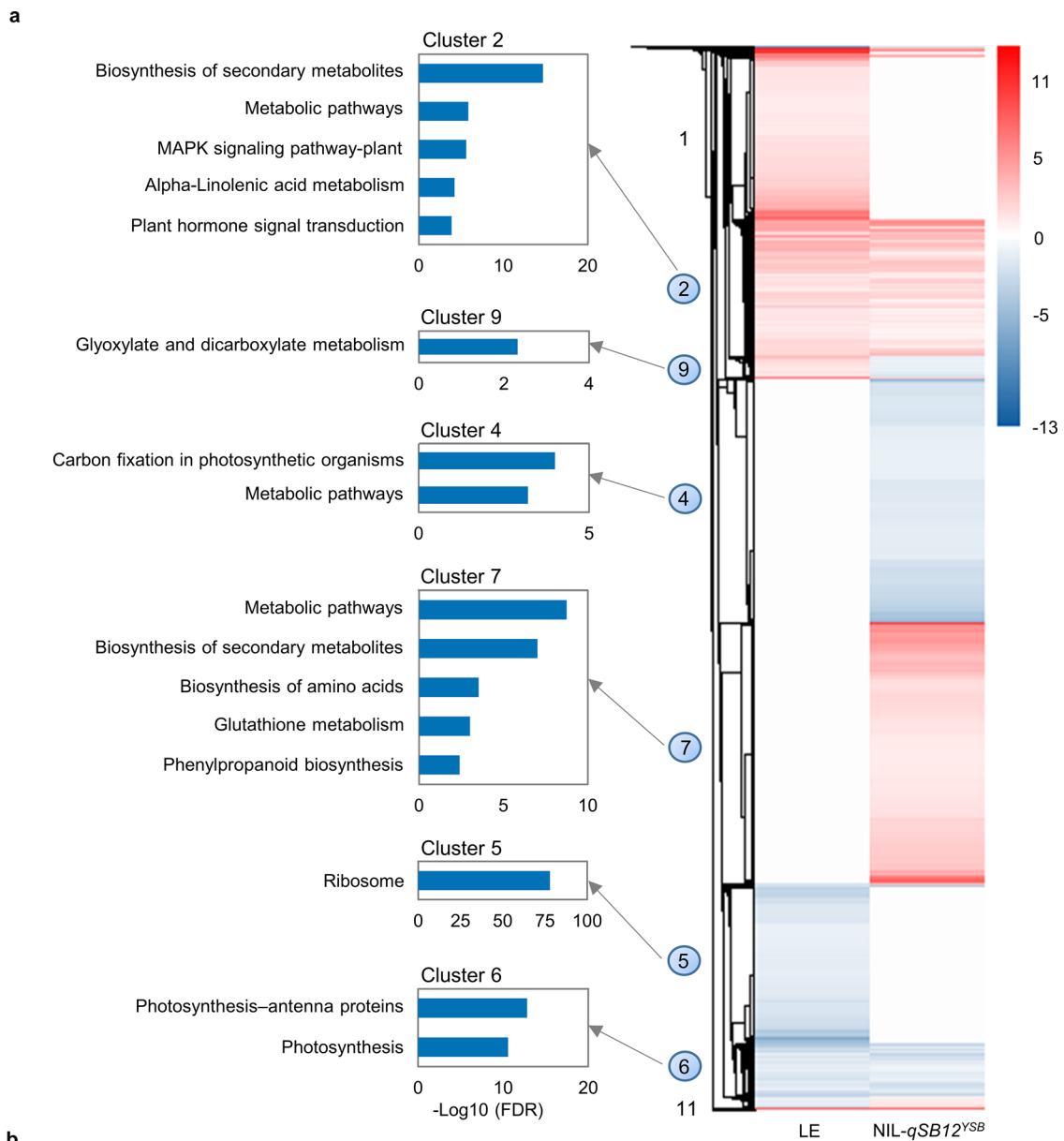


Fig. 4 Transcriptomic analysis of differentially expressed genes regulated by *qSB12^{YSB}*. **a** Hierarchical clustering and heatmap of 2326 differential expressed genes in response to *R.solani* and their related KEGG pathways. The differential expressed genes are grouped into 11 co-expressed clusters. Colors represent log₂-fold change comparing relative expression. **b, c, d** The relative expression levels of genes involved in cell redox homeostasis, carbon fixation and OPPP in LE and NIL-*qSB12^{YSB}* after inoculation. Colors represent log₂-fold change comparing relative expression. G6PD, glucose-6-phosphate dehydrogenase; PGL, 6-phosphogluconolactonase; 6PGDH, 6-phosphogluconate dehydrogenase. **e** DAB staining results of inoculated LE and NIL-*qSB12^{YSB}* leaves at 20 HAI

namely, ARF25, encodes an auxin response factor. Suppressing ARFs by targeting with miR167 reduced rice resistance to *Magnaporthe oryzae* (Zhao et al. 2020). *Os12g0614000* encodes mediator subunit 19a (MED19a). Mediator plays important roles in plant development and resistance (Kidd et al. 2011). AtMED19a, the homologue of OsMED19a, regulates resistance to biotrophic and hemi-biotrophic pathogens. Degradation of AtMED19a led to downregulation of the SA signaling pathway while upregulation of the JA/ET signaling pathway (Caillaud et al. 2013). *Os12g0616000* encodes a kinesin motor domain containing protein. A kinesin-like protein (KLP) has been shown a role in promoting ShB resistance via activation of auxin redistribution and subsequent activation of auxin signaling (Chu et al. 2021). *Os12g0614900*, *Os12g0615200*, *Os12g0615300* all encode wall-associated kinases (WAK) named OsWAK127b, OsWAK129c, OsWAK129b, respectively. WAKs play important roles in both plant development and pathogen response (Kohorn & Kohorn 2012). *Os12g0616200* encodes a ribosomal protein. Ribosomal proteins are major components of ribosomes involved in the cellular process of protein biosynthesis and play a minor role in basal resistance against virulent pathogens. GhARPL18A-6 (ribosomal protein L18A) can induce lignin deposition, ROS bursts and phenylpropanoid biosynthesis defense response pathways to increase resistance to *Verticillium dahlia* (Zhang et al. 2019). *Os12g0616500* encodes a cation/H⁺ exchanger protein. Cation/H⁺ exchangers play an important role in response to abiotic stresses in plants (Pandey 2015). *Os12g0616600* encodes a putative Deg protease homologue. Deg protease plays an important role in the photosystem II repair cycle under light stress condition (Kapri-pardes et al. 2007). *Os12g0616900* encodes a transketolase (TK). TK catalyzes reactions in the Calvin cycle and OPPP. Upregulation of TKs would produce more

erythrose-4-phosphate (E4P), which is a precursor for the shikimate pathway, leading to enhanced phenylpropanoid biosynthesis (Henkes et al. 2001). Upregulation of OPPP would also provide more NADPH to inhibit oxidative bursts (Linnenbrügger et al. 2022). These most likely candidates for *qSB12^{YSB}* have been cloned for functional verification through gene knock out and overexpression.

A number of studies have shown that pathogens often attack and disrupt plant photosynthetic systems, especially photosystem II complex, to promote pathogenesis (Serrano et al. 2016; Torres-Zabala et al. 2015). Recently, Ghosh et al. (2017) found that *R. solani* infection can destroy chloroplasts and inhibit photosynthesis in rice. The inhibition of photosynthesis will produce less NADPH and cause production of excess ROS in plants (Gan et al. 2019). In general, ROS has a dual function in regulating plant defenses. In plant-biotrophs/hemibiotrophs interactions, ROS functions as a signal molecule to initiate defense responses against fungal pathogens (Kou et al. 2019), and therefore, host-derived ROS can inhibit further expansion of pathogen to adjacent cells (Liu et al. 2014). To inhibit host ROS-dependent immunity, pathogens activate their antioxidation systems and block host ROS bursts to facilitate pathogenicity (Molina and Kahmann 2007; Liu and Zhang 2022). On the contrary, in plant-necrotrophs interactions, necrotrophic pathogens often stimulate excessive ROS accumulation in the host to induce cell death, which is conducive to the growth and colonization of necrotrophic fungi, while the host may activate antioxidation systems to inhibit ROS bursts induced by the pathogen (Heller and Tudzynski 2011). In rice-*R. solani* interaction, several lines of evidences have been shown to support this hypothesis. Our ShB resistant line exhibits a significantly lower ROS accumulation compared with the susceptible control at 48 h post inoculation with *R. solani*, further supporting the above hypothesis. Similarly, QTL *qLN11* indirectly activates genes involved in the ROS-redox pathway, alleviates ROS accumulation in rice cells, and thus delays *R. solani* colonization (Oreiro et al. 2022). Disease resistance protein OsRSR1 and protein kinase OsRLCK5 are involved in sheath blight resistance by regulating ROS levels through the glutathione-ascorbic acid antioxidant system (Wang et al. 2021). Suppression of *R. solani*-induced rice chlorophyll degradation improves rice ShB resistance via reducing *R. solani*-induced ROS bursts (Cao et al. 2022).

Here, we present a model for *qSB12^{YSB}*-mediated ShB resistance to summarize our results (Fig. 6). *R. solani* attacks host photosynthetic systems to promote pathogenesis during

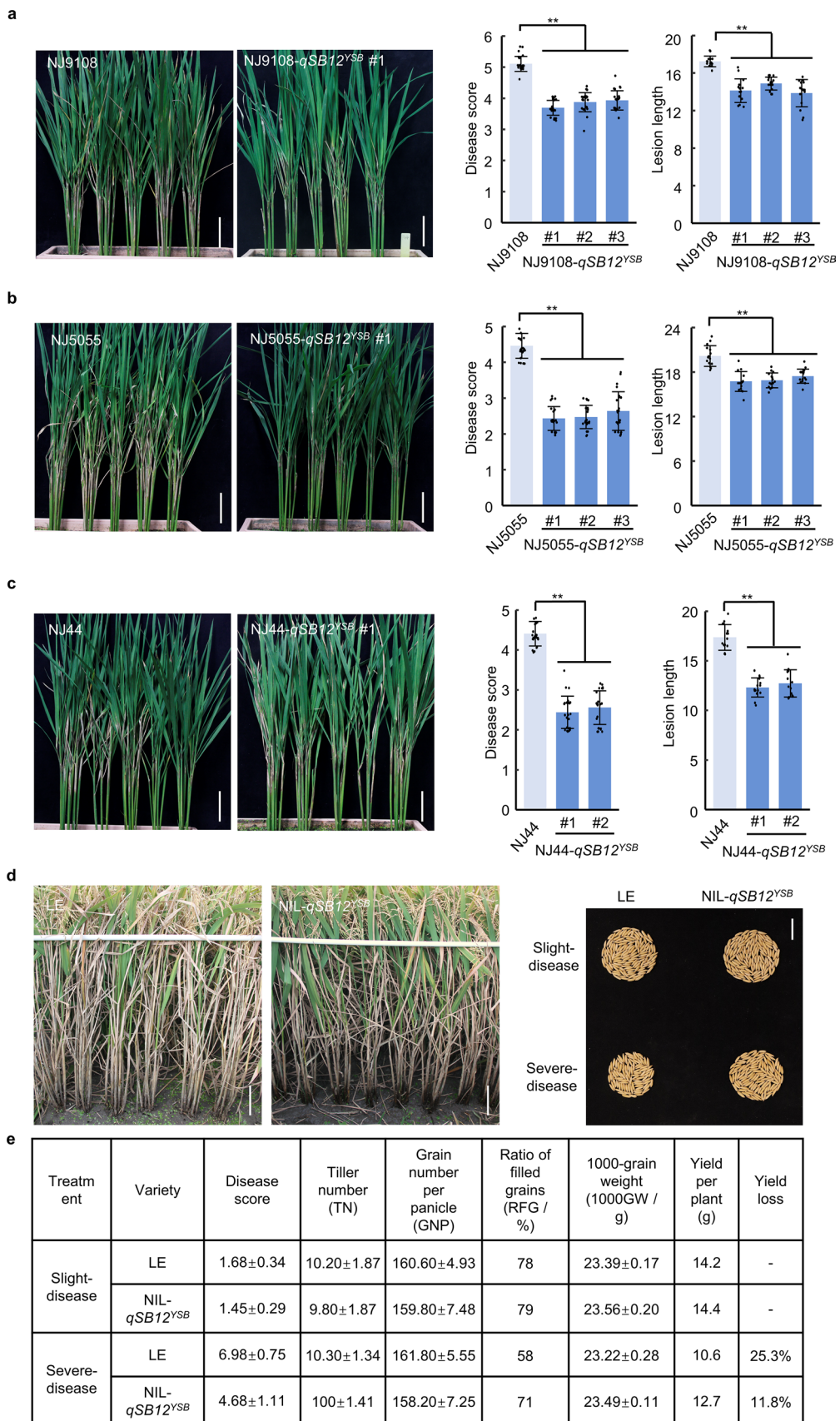


Fig. 5 Breeding potential of *qSB12^{YSB}* in improving sheath blight resistance. **a, b, c** Disease phenotypes of NJ9108 (**a**), NJ5055 (**b**), NJ44 (**c**) and their respective *qSB12^{YSB}* introgression lines in field and greenhouse tests. Images showed the phenotype in 14DAI in green house. ****P**<0.01 using Student’s *t*-test. Scale bar, 10 cm. **d** Disease severity and yields of LE and NIL-*qSB12^{YSB}* after ShB inoculation. The LE and NIL-*qSB12^{YSB}* lines were planted for yield tests under two different ShB disease conditions: non-disease to severe-disease conditions. Each test contained 3 replications per line for LE and NIL-*qSB12^{YSB}*. A total of 300 plants for each line were harvested and the yield measured. The filled grains in the main panicle were collected and photographed. **e** ShB resistance and morphological traits of LE and NIL-*qSB12^{YSB}*. Disease score, tiller number (TN), and grain number per main panicle (GNP) were measured from 10 plants per line. Values are means±SD (*n*=10 plants). 1000-grain weight (1000GW) was measured from three replications, Values are means±SD (*n*=3 plants). Yield per plant was measured from 300 plants

infection. Inhibition of host photosynthesis causes lower levels of NADPH that affects cell redox balance, leading to cell death due to excess ROS. NIL-*qSB12^{YSB}* initiates three steps to counter excess ROS to protect plants from the oxidative damage. First, *qSB12^{YSB}* slows down the Calvin-Benson cycle freeing reducing power to cope with increased oxidants. Second, *qSB12^{YSB}* activates OPPP to produce more NADPH. Third, *qSB12^{YSB}* activates expression of cell redox genes to maintain ROS homeostasis to prevent cell death. These three steps help NIL-*qSB12^{YSB}* counter the ROS bursts induced by *R. solani* infection. In addition, NIL-*qSB12^{YSB}* also activates the glycolysis pathway and the phenylpropanoid pathway to produce more resistance-related secondary metabolites to defend against *R. solani*.

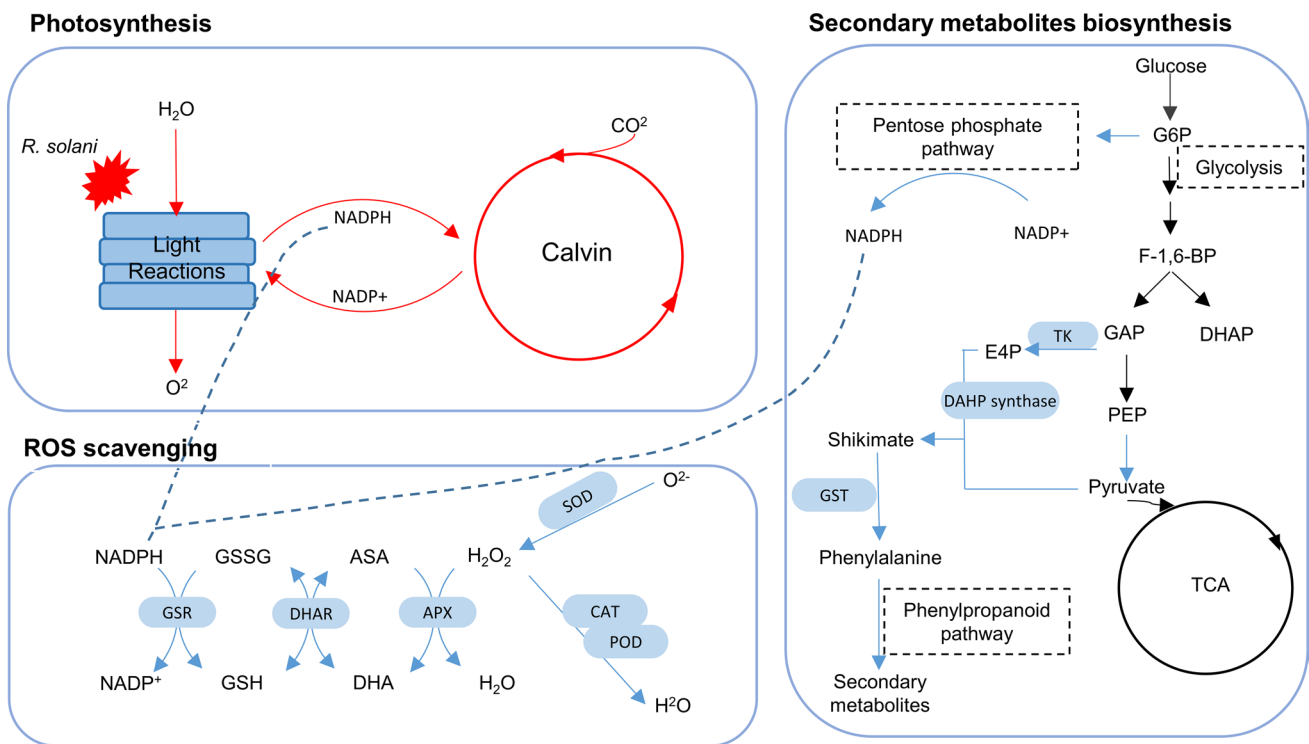


Fig. 6 Potential mechanisms of ShB resistance regulated by *qSB12^{YSB}*. Model of *qSB12^{YSB}*-mediated ShB resistance. *R. solani* attacks host photosynthetic systems to promote pathogenesis during infection, inducing plant cell death due to excessive ROS. To protect plants from the oxidative damage, *qSB12^{YSB}* slows down the Calvin-Benson cycle and activates OPPP to improve NADPH level in plants. *qSB12^{YSB}* also activates cell redox-related genes to maintain

ROS homeostasis to reduce cell death. These three steps finally help NIL-*qSB12^{YSB}* to inhibit ROS bursts induced by *R. solani* infection. *qSB12^{YSB}* also activates the glycolysis and phenylpropanoid pathways to produce more resistance-related secondary metabolites to defend against *R. solani*. Red lines represent the down expressed pathways. Blue lines represent the up expressed pathways. Black lines represent the pathways none differentially expressed pathway

Supplementary Information The online version contains supplementary material available at <https://doi.org/10.1007/s00122-023-04482-z>.

Acknowledgements We thank Dr. Mawsheng Chern (University of California, Davis, USA) for polishing the manuscript language. This study was supported by the National Natural Science Foundation of China (31872858 and 32000362), Seed Industry Revitalization Project of Jiangsu Province (JBGS2021001), Natural Science Foundation of Jiangsu Province (BK20200930), the "333" High-level Personnel Training Project of Jiangsu Province, Jiangsu Safety & Environment Technology and Equipment for Planting and Breeding Industry Engineering Research and Application of Excellent Science and Technology Innovation Team Project and a Project Funded by Priority Academic Program Development of Jiangsu Higher Education Institutions (PAPD).

Authors contribution statement SZ conceived the project; YW performed the experiments; QS, TL, HD, WS and KW assisted in phenotyping and genotyping of the populations; JZ assisted in analyzing the resequencing and RNA-seq data; CY and JL assisted in detecting some enzymes' activities; XX, ZC, KH, ZF, SZ assisted in revising the manuscript; YW and SZ analyzed the experimental results and wrote the manuscript. All authors have read and approved the final manuscript.

Funding This study was partially supported by the National Natural Science Foundation of China (31872858 and 32000362), Seed Industry Revitalization Project of Jiangsu Province (JBGS2021001), Natural Science Foundation of Jiangsu Province (BK20200930), the "333" High-level Personnel Training Project of Jiangsu Province, and a Project Funded by Priority Academic Program Development of Jiangsu Higher Education Institutions (PAPD), respectively.

Data availability The datasets generated or analyzed during this study are available from the corresponding author on reasonable request.

Declarations

Conflict of interest The authors declare that they have no conflict of interest.

References

- Anderson JP, Hane JK, Stoll T, Pain N, Hastie ML, Kaur P, Hoogland C, Gorman JJ, Singh KB (2016) Proteomic analysis of *Rhizoctonia solani* identifies infection-specific, redox associated proteins and insight into adaptation to different plant hosts. *Mol Cell Proteomics* 15:1188–1203. <https://doi.org/10.1074/mcp.M115.054502>
- Bollich CN, Webb BD, Marchetti MA, Scott JE (1985) Registration of 'Lemont' rice. *Crop Sci* 25:883–885. <https://doi.org/10.2135/cropsci1985.0011183x002500050038x>
- Caillaud MC, Asai S, Rallapalli G, Piquerez S, Fabro G, Jones JDG (2013) A downy mildew effector attenuates salicylic acid-triggered immunity in Arabidopsis by interacting with the host mediator complex. *PLoS Biol* 11:e1001732. <https://doi.org/10.1371/journal.pbio.1001732>
- Cao WL, Zhang HM, Zhou Y, Zhao JH, Lu SB, Wang XQ, Yuan LM, Guan HY, Wang GD, Shen WX, De Vleeschauwer D, Li ZQ, Shi XP, Gu JF, Guo M, Feng ZM, Chen ZX, Zhang YF, Pan XB, Zuo SM (2022) Suppressing chlorophyll degradation by silencing *OsNYC3* improves rice resistance to *Rhizoctonia solani*, the causal agent of sheath blight. *Plant Biotechnol J* 20:335–349. <https://doi.org/10.1111/pbi.13715>

- Channamallikarjuna V, Sonah H, Prasad M, Rao GJN, Chand S, Upreti HC, Singh NK, Sharma TR (2010) Identification of major quantitative trait loci *qSBR11-1* for sheath blight resistance in rice. *Mol Breeding* 25:155–166. <https://doi.org/10.1007/s11032-009-9316-5>
- Chen ZX, Zhang YF, Feng F, Feng MH, Jiang W, Ma YY, Pan CH, Hua HL, Li GS, Pan XB, Zuo SM (2014) Field crops research improvement of *japonica* rice resistance to sheath blight by pyramiding *qSB-9^{TQ}* and *qSB-7^{TQ}*. *Field Crop Res* 161:118–127. <https://doi.org/10.1016/j.fcr.2014.03.003>
- Chu J, Xu H, Dong H, Xuan YH (2021) Loose plant architecture 1-Interacting kinesin-like protein KLP promotes rice resistance to sheath blight disease. *Rice* 14:60. <https://doi.org/10.1186/s12284-021-00505-9>
- Cu RM, Mew TW, Cassman KG, Teng PS (1996) Effect of sheath blight on yield in tropical, intensive rice production system. *Plant Dis* 80:1103–1108. <https://doi.org/10.1094/PD-80-1103>
- Eizenga GC, Jia MH, Pinson SR, Gasore ER, Prasad B (2015) Exploring sheath blight quantitative trait loci in a Lemont/*O. meridionalis* advanced backcross population. *Mol Breed* 35:1–19. <https://doi.org/10.1007/s11032-015-0332-3>
- Foley RC, Kidd BN, Hane JK, Anderson JP, Singh KB (2016) Reactive oxygen species play a role in the infection of the necrotrophic fungi. *Rhizoctonia Solani* in Wheat *Plos One* 11:e015254816. <https://doi.org/10.1371/journal.pone.0152548>
- Gan P, Liu F, Li R, Wang SK, Luo JJ (2019) Chloroplasts-beyond energy capture and carbon fixation: tuning of photosynthesis in response to chilling stress. *Int J Mol Sci* 20:5046. <https://doi.org/10.3390/ijms20205046>
- Ghosh S, Kanwar P, Jha G (2017) Alterations in rice chloroplast integrity, photosynthesis and metabolome associated with pathogenesis of *Rhizoctonia solani*. *Sci Rep* 6:41610. <https://doi.org/10.1038/srep41610>
- Gnanamanickam SS (2009) Biological control of rice diseases. In *Progress in biological control*. Vol 8, pp 79–89. <https://doi.org/10.1007/978-90-481-2465-7>
- He M, Yin JJ, Feng ZM, Zhu XB, Zhao JH, Zuo SM, Chen XW (2020) Methods for evaluation of rice resistance to blast and sheath blight diseases. *Chin Bull Bot* 55:577–587. <https://doi.org/10.11983/CBB20100>
- Heller J, Tudzynski P (2011) Reactive oxygen species in phytopathogenic fungi: signaling, development, and disease. *Annu Rev Phytopathol* 49:369–390. <https://doi.org/10.1146/annurev-phyto-072910-095355>
- Henkes S, Sonnwald U, Badur R, Flachmann R, Stitt M (2001) A small decrease of plastid transketolase activity in antisense tobacco transformants has dramatic effects on photosynthesis and phenylpropanoid metabolism. *Plant Cell* 13:535–551. <https://doi.org/10.1105/tpc.13.3.535>
- Kapri-pardes E, Naveh L, Adam Z (2007) The thylakoid lumen protease Deg1 is involved in the repair of photosystem II from photoinhibition in Arabidopsis. *Plant Cell* 19:1039–1047. <https://doi.org/10.1105/tpc.106.046573>
- Kidd BN, Cahill DM, Manners JM, Schenk PM, Kazan K (2011) Diverse roles of the mediator complex in plants. *Semin Cell & Dev Biol* 21:741–748. <https://doi.org/10.1016/j.semcdb.2011.07.012>
- Kim P, Xu CY, Song HD, Gao Y, Feng L, Li YH, Xuan YH (2021) Tissue-specific activation of DOF11 promotes rice resistance to sheath blight disease and increases grain weight via activation of SWEET14. *Plant Biotechnol J* 19:409–411. <https://doi.org/10.1111/pbi.13489>
- Kohorn BD, Kohorn SL (2012) The cell wall-associated kinases, WAKs, as pectin receptors. *Front Plant Sci* 3:88. <https://doi.org/10.3389/fpls.2012.00088>



- Kou YJ, Qiu JH, Tao Z (2019) Every coin has two sides: reactive oxygen species during rice-*Magnaporthe oryzae* interaction. *Int J Mol Sci* 20:1191. <https://doi.org/10.3390/ijms20051191>
- Lee NF, Rush MC (1983) Rice sheath blight: a major rice disease. *Plant Dis* 6:829–832. <https://doi.org/10.1094/PD-67-829>
- Li ZK, Pinson SRM, Marchetti MA, Stansel JW, Park WD (1995a) Characterization of quantitative trait loci (QTLs) in cultivated rice contributing to field resistance to sheath blight (*Rhizoctonia solani*). *Theor Appl Genet* 91:382–388. <https://doi.org/10.1007/BF00220903>
- Li MY, Wang JN, Wang GD, Feng ZM, Ye YH, Jiang W, Zuo T, Zhang YF, Chen XJ, Pan XB, Ma YY, Chen ZX, Zuo SM (2019a) Improvement of *japonica* rice resistance to sheath blight disease by incorporating quantitative resistance genes *qSB-11^{HJX}* and *qSB-9^{QE}*. *J Yangzhou Univ (agric Life Sci Ed)* 40:7. <https://doi.org/10.16872/j.cnki.1671-4652.2019.06.001>
- Li ZK, Pinson SRM, Stansel JW, Park WD (1995b) Identification of quantitative trait loci (QTLs) for heading date and plant height in cultivated rice (*Oryza sativa* L.). *Theor Appl Genet* 91:374–381. <https://doi.org/10.1007/BF00220902>
- Li N, Lin B, Wang H, Li XM, Yang FF, Ding XH, Yan JB, Chu ZH (2019b) Natural variation in *ZmFBL41* confers banded leaf and sheath blight resistance in maize. *Nat Genet* 51:1540–1548. <https://doi.org/10.1038/s41588-019-0503-y>
- Li DY, Li S, Wei SH, Sun WX (2021) Strategies to manage rice sheath blight: lessons from interactions between rice and *Rhizoctonia solani*. *Rice* 14:21. <https://doi.org/10.1186/s12284-021-00466-z>
- Linnenbrügger L, Doering L, Lansing H, Fischer K, Eirich J, Finke-meier I, Von Schaeuwen A (2022) Alternative splicing of Arabidopsis G6PD5 recruits NADPH-producing OPPP reactions to the endoplasmic reticulum. *Front Plant Sci* 13:909624. <https://doi.org/10.3389/fpls.2022.909624>
- Liu XY, Zhang ZG (2022) A double-edged sword: reactive oxygen species (ROS) during the rice blast fungus and host interaction. *FEBS J* 289:5505–5515. <https://doi.org/10.1111/febs.16171>
- Liu WD, Liu JL, Triplett L, Leach JE, Wang GL (2014) Novel insights into rice innate immunity against bacterial and fungal pathogens. *Annu Rev Phytopathol* 52:213–241. <https://doi.org/10.1146/annurev-phyto-102313-045926>
- Michelet L, Zaffagnini M, Marchand C, Collin V, Decottignies P, Tsan P, Lancelin JM, Trost P, Miginiac-Maslow M, Noctor G, Lemaire SD (2005) Glutathionylation of chloroplast thioredoxin f is a redox signaling mechanism in plants. *Proc Natl Acad Sci USA* 102:16478–16483. <https://doi.org/10.1073/pnas.0507498102>
- Michelet L, Zaffagnini M, Massot V, Keryer E, Vanacker H, Miginiac-Maslow M, Issakidis-Bourguet E, Lemaire SD (2006) Thioredoxins, glutaredoxins, and glutathionylation: new crosstalks to explore. *Photosynth Res* 89:225–245. <https://doi.org/10.1007/s11120-006-9096-2>
- Michelet L, Zaffagnini M, Morisse S, Sparla F, Pérez-Pérez ME, Francia F, Danon A, Marchand CH, Fermani S, Trost P, Lemaire SD (2013) Redox regulation of the Calvin–Benson cycle: something old, something new. *Front Plant Sci* 4:470. <https://doi.org/10.3389/fpls.2013.00470>
- Molina L, Kahmann R (2007) An *Ustilago maydis* gene involved in H₂O₂ detoxification is required for virulence. *Plant Cell* 19:2293–2309. <https://doi.org/10.1105/tpc.107.052332>
- Molla KA, Karmakar S, Molla J, Bajaj P, Varshney RK, Datta SK, Datta K (2020) Understanding sheath blight resistance in rice: the road behind and the road ahead. *Plant Biotechnol J* 18:895–915. <https://doi.org/10.1111/pbi.13312>
- Mutuku JM, Nose A (2012) Changes in the contents of metabolites and enzyme activities in rice plants responding to *Rhizoctonia solani* kühn infection: activation of glycolysis and connection to phenylpropanoid pathway. *Plant Cell Physiol* 53:1017–1032. <https://doi.org/10.1093/pcp/pcs047>
- Oreiro EG, Grimares EK, Grande G, Quibod IL, Roman-Reyna V, Oliva R (2022) Genome-wide associations and transcriptional profiling reveal ROS regulation as one underlying mechanism of sheath blight resistance in rice. *Mol Plant Microbe Interact* 33:212–222. <https://doi.org/10.1094/MPMI-05-19-0141-R>
- Pan XB, Rush MC, Sha XY, Xie QJ, Oard JH (1999) Major gene, non-allelic sheath blight resistance from the rice cultivars Jasmine 85 and Teqing. *Crop Sci* 39:338–346. <https://doi.org/10.2135/cropsci1999.0011183x003900020006x>
- Pandey GK (2015) Elucidation of abiotic stress signaling in plants: functional genomics perspectives. Springer, New York Heidelberg Dordrecht, London. <https://doi.org/10.1007/978-1-4939-2211-6>
- Pinson SRM, Capdevielle FM, Oard JH (2005) Confirming QTLs and finding additional loci conditioning sheath blight resistance in rice using recombinant inbred lines. *Crop Sci* 45:503–510. <https://doi.org/10.2135/cropsci2005.0503>
- Porebski S, Bailey LG, Baum BR (1997) Modification of a CTAB DNA extraction protocol for plants containing high polysaccharide and polyphenol components. *Plant Mol Biol Report* 15:8–15. <https://doi.org/10.1007/BF02772108>
- Savary S, Castilla NP, Elazegui FA, McLaren CG, Ynalvez MA, Teng PS (1995) Direct and indirect effects of nitrogen supply and disease source structure on rice sheath blight spread. *Phytopathology* 85:959–965. <https://doi.org/10.1094/Phyto-85-959>
- Scharte J, Schön H, Tjaden Z, Weis E, Von Schaeuwen A (2009) Isoenzyme replacement of glucose-6-phosphate dehydrogenase in the cytosol improves stress tolerance in plants. *Proc Natl Acad Sci USA* 106:8061–8066. <https://doi.org/10.1073/pnas.0812902106>
- Schürmann P, Buchanan BB (2008) The ferredoxin/thioredoxin system of oxygenic photosynthesis. *Antioxid Redox Signal*. <https://doi.org/10.1089/ars.2007.1931>
- Serrano I, Audran C, Rivas S (2016) Chloroplasts at work during plant innate immunity. *J Exp Bot* 67:3845–3854. <https://doi.org/10.1093/jxb/erw088>
- Shetty NP, Jørgensen HJL, Jensen JD, Collinge DB, Shetty HS (2008) Roles of reactive oxygen species in interactions between plants and pathogens. *Eur J Plant Pathol* 121:267–280. <https://doi.org/10.1007/s10658-008-9302-5>
- Srinivasachary WL, Savary S (2011) Resistance to rice sheath blight (*Rhizoctonia solani* Kühn [(teleomorph: *Thanatephorus cucumeris* (A. B. Frank) Donk] disease: current status and perspectives. *Euphytica* 178:1–22. <https://doi.org/10.1007/s10681-010-0296-7>
- Taguchi-Shiobara F, Ozaki H, Sato H, Maeda H, Kojima Y, Ebitani T, Yano M (2013) Mapping and validation of QTLs for rice sheath blight resistance. *Breed Sci* 63:301–308. <https://doi.org/10.1270/jsbbs.63.301>
- Torres-Zabala MD, Littlejohn G, Jayaraman S, Studholme D, Bailey T, Lawson T, Tillich M, Licht D, Böller B, Delfino L, Truman W, Mansfield J, Smirnoff N, Grant M (2015) Chloroplasts play a central role in plant defence and are targeted by pathogen effectors. *Nature Plants* 1:15074–15111. <https://doi.org/10.1038/NPLANT.2015.74>
- Wang CL, Zhang YD, Zhu Z, Zhao L, Zhong WG, Chen ZD, Yang J (2007) Breeding and utilization of a new rice variety Nanjing 44 with resistance to stripe blight. *China Rice* 2:33–34. <https://doi.org/10.3969/j.issn.1006-8082.2007.02.010>
- Wang CL, Zhang YD, Zhu Z, Chen T, Zhao QY, Zhao L, Zhou LH, Yao S (2012) Breeding and utilization of new *japonica* rice variety Nanjing 5055 with good Taste. *Bull Agric Sci Technol* 02:84–88. <https://doi.org/10.3969/j.issn.1000-6400.2012.02.039>
- Wang CL, Zhang YD, Zhu Z, Yao S, Zhao QY, Chen T, Zhou LH, Zhao L (2013) Breeding and utilization of new *japonica* rice variety

- Nanjing 9108 with good taste. *Jiangsu Agric Sci* 41:86–88. <https://doi.org/10.15889/j.issn.1002-1302.2013.09.108>
- Wang AJ, Shu XY, Jing X, Jiao CZ, Chen L, Zhang JF, Ma L, Jiang YQ, Yamamoto N, Li SC, Deng QM, Wang SQ, Zhu J, Liang YY, Zou T, Liu HN, Wang LX, Huang YB, Li P, Zheng AP (2021) Identification of rice (*Oryza sativa* L.) genes involved in sheath blight resistance via a genome-wide association study. *Plant Biotechnol J* 19:1553–1566. <https://doi.org/10.1111/pbi.13569>
- Zhang YH, Jin YY, Gong Q, Li Z, Zhao LH, Han X, Zhou JL, Li FG, Yang ZE (2019) Mechanism analysis of resistance to *Verticillium dahliae* in upland cotton conferred by overexpression of RPL18A-6 (Ribosomal Protein L18A-6). *Ind Crops Prod* 141:111742. <https://doi.org/10.1016/j.indcrop.2019.111742>
- Zhao ZX, Feng Q, Cao XL, Zhu Y, Wang H, Chandran V, Fan J, Zhao JQ, Pu M, Li Y, Wang WM (2020) *Osa-miR167d* facilitates infection of *Magnaporthe oryzae* in rice. *J Integr Plant Biol* 62:702–715. <https://doi.org/10.1111/jipb.12816>
- Zhu YJ, Zuo SM, Chen ZX, Chen XG, Li G, Zhang YF, Zhang GQ, Pan XB (2014) Identification of two major rice sheath blight resistance QTLs, *qSB1-1^{HJX74}* and *qSB11^{HJX74}*, in field trials using chromosome segment substitution lines. *Plant Dis* 98:1112–1121. <https://doi.org/10.1094/PDIS-10-13-1095-RE>
- Zou JH, Pan XB, Chen ZX, Xu JY, Lu JF, Zhai WX, Zhu LH (2000) Mapping quantitative trait loci controlling sheath blight resistance in two rice cultivars (*Oryza sativa* L.). *Theor Appl Genet* 101:569–573. <https://doi.org/10.1007/s001220051517>
- Zuo SM, Wang ZB, Chen XJ, Gu F, Zhang YF, Chen ZX, Pan XB (2009) Evaluation of resistance of a novel rice germplasm YSBR1 to sheath blight. *Acta Agron Sin* 35:608–614. <https://doi.org/10.3724/sp.j.1006.2009.00608>
- Zuo SM, Yin YJ, Pan CH, Chen ZX, Zhang YF, Gu SL, Zhu LH, Pan XB (2013) Fine mapping of *qSB-11^{LE}*, the QTL that confers partial resistance to rice sheath blight. *Theor Appl Genet* 126:1257–1272. <https://doi.org/10.1007/s00122-013-2051-7>
- Zuo SM, Zhang YF, Yin YJ, Li G, Zhang GW, Wang H, Chen ZX, Pan XB (2014) Fine-mapping of *qSB-9TQ*, a gene conferring major quantitative resistance to rice sheath blight. *Mol Breed* 34:2191–2203. <https://doi.org/10.1007/s11032-014-0173-5>

Publisher's Note Springer Nature remains neutral with regard to jurisdictional claims in published maps and institutional affiliations.

Springer Nature or its licensor (e.g. a society or other partner) holds exclusive rights to this article under a publishing agreement with the author(s) or other rightsholder(s); author self-archiving of the accepted manuscript version of this article is solely governed by the terms of such publishing agreement and applicable law.

Authors and Affiliations

Yu Wang¹ · Quanyi Sun¹ · Jianhua Zhao¹ · Taixuan Liu¹ · Haibo Du¹ · Wenfeng Shan¹ · Keting Wu¹ · Xiang Xue^{4,5} · Chao Yang⁶ · Jun Liu⁶ · Zongxiang Chen^{1,2} · Keming Hu^{1,2} · Zhiming Feng^{1,2}  · Shimin Zuo^{1,2,3} 

✉ Zhiming Feng
fengzm@yzu.edu.cn

✉ Shimin Zuo
smzuo@yzu.edu.cn

Yu Wang
861911991@qq.com

Quanyi Sun
sunquanyi2023@163.com

Jianhua Zhao
1145757247@qq.com

Taixuan Liu
1015323109@qq.com

Haibo Du
18703736901@163.com

Wenfeng Shan
shanwenfeng@sjtu.edu.cn

Keting Wu
53990345@qq.com

Xiang Xue
476530460@qq.com

Chao Yang
chaoyang@cau.edu.cn

Jun Liu
junliu@im.ac.cn

Zongxiang Chen
czx@yzu.edu.cn

Keming Hu
hukm@yzu.edu.cn

- 1 Jiangsu Key Laboratory of Crop Genomics and Molecular Breeding/Zhongshan Biological Breeding Laboratory/Key Laboratory of Plant Functional Genomics of the Ministry of Education, Agricultural College of Yangzhou University, Yangzhou 225009, People's Republic of China
- 2 Co-Innovation Center for Modern Production Technology of Grain Crops of Jiangsu Province/Key Laboratory of Crop Genetics and Physiology of Jiangsu Province, Yangzhou University, Yangzhou 225009, People's Republic of China
- 3 Joint International Research Laboratory of Agriculture and Agri-Product Safety, Ministry of Education of China/Institutes of Agricultural Science and Technology Development, Yangzhou University, Yangzhou 225009, People's Republic of China
- 4 Yangzhou Polytechnic College, Yangzhou 225009, People's Republic of China
- 5 Jiangsu Safety and Environment Technology and Equipment for Planting and Breeding Industry Engineering Research Center, Yangzhou Polytechnic College, Yangzhou 225009, People's Republic of China
- 6 MOA Key Laboratory of Pest Monitoring and Green Management, College of Plant Protection, China Agricultural University, Beijing 100193, People's Republic of China